Pediatr Radiol (2011) 41:1308–1320
DOI 10.1007/s00247-011-2119-y

PICTORIAL ESSAY

MRI of closed spinal dysraphisms

Chaitra A. Badve · Paritosh C. Khanna · Grace S. Phillips · Mahesh M. Thapa · Gisele E. Ishak

Received: 11 February 2011 / Revised: 3 April 2011 / Accepted: 12 April 2011 / Published online: 19 May 2011

Abstract We present a pictorial review of MRI features of various closed spinal dysraphisms based on previously described clinicoradiological classification of spinal dysraphisms proposed. The defining imaging features of each dysraphism type are highlighted and a diagnostic algorithm for closed spinal dysraphisms is suggested.

Keywords Spinal dysraphism · MRI · Lipomyelomeningocele · Myelocystocele

Introduction

The term "spinal dysraphism" includes a spectrum of congenital fusion anomalies of one or more dorsal midline structures including skin, subcutaneous tissue, vertebrae, meninges and neural tissue. Initial clinical descriptions of spinal dysraphism were made by Lichtenstein [1] in 1940 and James and Lassman [2] in 1960. Early imaging approaches were based on the use of conventional radiography, US and CT [3, 4]. MRI of spinal dysraphism was described by Barnes et al. [5].

CME activity
This article has been selected as the CME activity for the current month. Please visit the SPR website at www.pedrad.org on the Education page and follow the instructions to complete this CME activity.

C. A. Badve · P. C. Khanna · G. S. Phillips · M. M. Thapa · G. E. Ishak (✉)
Department of Radiology, Seattle Children's Hospital and University of Washington Medical Center,
4800 Sand Point Way NE,
Seattle, WA 98105, USA
e-mail: ishakg@u.washington.edu

A comprehensive report in 2000 by Tortori-Donati and coworkers [6] proposed an effective working classification of spinal dysraphisms. Based on clinical and imaging features, this classification helped in characterizing each form of spinal dysraphism. In spite of this pioneering work, the topic of spinal dysraphism continues to pose significant challenges to beginners in pediatric neuroradiology. This pictorial review illustrates the MR characteristics of various types of closed spinal dysraphisms based on the classification presented by Tortori-Donati et al. [6]. Our categorization leads to a simple diagnostic algorithm for closed spinal dysraphism.

Epidemiology

The worldwide incidence of neural tube defects ranges between 1.0 and 10.0 per 1,000 births, with almost half of these cases falling under the category of spinal dysraphisms and the other half consisting of anencephaly cases [7]. The prevalence of spinal dysraphisms in the United States in 2005 was about two per 10,000 live births. Variations in prevalence based on race, ethnicity, gender and region have also been reported [8, 9]. The prevalence of neural tube defects (including anencephaly and spinal dysraphisms) has been on the decline during the last 25 years as a result of antenatal screening and folic acid supplementation [10].

Embryology

Neural tube development is a complex process involving multiple steps occurring between 2 and 6 weeks of

intrauterine life [11–13]. The important steps in this process are:

Gastrulation: A trilaminar disc consisting of a layer of future mesoderm (mesoblast) sandwiched between layers of future ectoderm (epiblast) and endoderm (hypoblast) is created. The notochord is formed in the midline along the dorsal surface of the embryo. Anomalies such as caudal regression syndrome, diastematomyelia, neurenteric cyst and dorsal enteric fistula occur because of aberrations during gastrulation [14].

Primary neurulation: The notochord induces the surface ectoderm to form neuroectoderm. The neuroectoderm transforms into a neural plate, then into a neural groove, and finally an enclosed neural tube. The neural tube separates from the surface ectoderm by a process called disjunction. The interface between the surface ectoderm (i.e. future skin layer) and the neural tube (i.e. future spinal cord) is occupied by mesenchymal cells (i.e. future meninges, vertebral arches and paraspinal muscles). Premature disjunction results in anomalies such as lipomyelocele, lipomyelomeningocele and intradural lipomas. Incomplete disjunction of neuroectoderm from surface ectoderm is believed to be the cause of dermal sinus [14].

Secondary neurulation and retrogressive differentiation: This process involves formation of the conus and the filum terminale from a secondary neural tube, which develops distal to the primary neural tube from the caudal cell mass. Aberrations in this process lead to anomalies such as filar lipoma, tight filum terminale and persistent terminal ventricle [14].

The paraxial mesoderm gives rise to somites, which further differentiate into deep skin layer, paraspinal muscles, intervertebral discs, ligaments and cartilage. In its early stages, the spinal cord is as long as the vertebral column; however, in the later stages the conus ascends in position and terminates at or above L2 [11].

Classification

Spinal dysraphism has been classified on the basis of embryological, embryopathogenetic, surgico-anatomical, neurological and imaging characteristics. As dysraphisms are developmental anomalies along a continuum, overlapping features often exist and analysis of two or more characteristics is necessary in neuroradiological diagnosis. Tortori-Donati et al. [6] proposed a clinico-radiological classification that combined clinical characteristics of an anomaly with its prominent radiological findings. Updates of this classification were published by Rossi and coworkers [14, 15], most recently in 2006. According to this classification, spinal dysraphism is broadly classified as *open* or *closed* based on the intactness of skin covering. Open spinal dysraphism has four variants: myelomeningocele, myeloschisis, hemimyelocele and hemimyelomeningocele, of which myelomeningocele is the most prevalent form. Closed spinal dysraphisms are further classified on the basis of presence or absence of a subcutaneous mass. A simplified adaptation of this classification is presented (Table 1).

Lumbosacral closed spinal dysraphisms with subcutaneous mass

Lipomyelocele and lipomyelomeningocele exhibit hypertrophy of subcutaneous fat with an associated dural defect. Another characteristic of these lesions is the presence of a neural placode. A neural placode consists of abnormal embryonic neural tissue and is seen in some closed and all open spinal dysraphisms. It can be seen involving the terminal most portion of the spinal cord, or, alternatively, it can be segmental in location with normal cord extending beyond the placode. The position of placode-lipoma interface and the width of the adjacent subarachnoid space help in differentiating lipomyelocele and lipomyelomeningocele. Terminal myelocystocele represents cystic expansion of the caudal central canal surrounded by expanded CSF subarachnoid space giving a cyst-within-cyst appearance. Meningocele is the simplest lesion of all and characteristically shows CSF-filled pachymeningeal herniation.

Lipomyelocele

Figure 1 shows a schematic representation of a lipomyelocele. The caudal portion of the spinal cord is composed of a neural placode. The placode is always terminal in location. The cord is often low-lying. The hypertrophic subcutaneous fat extends into the spinal canal through a large posterior spinal defect. The placode-lipoma interface can be focal or diffuse in extent, extending over several vertebral levels. However, the interface is always located within or at the edge of the spinal canal. There is no widening of the subarachnoid space (Fig. 1). The axial T1 images can play an important role in evaluating the placode-lipoma interface.

Lipomyelomeningocele

In a lumbosacral lipomyelomeningocele, the neural placode is often segmental in location, although a terminal placode can

Table 1 Classification of closed spinal dysraphism adapted from the clinico-neuroradiological classification by Tortori-Donati et al. [6, 14]

With subcutaneous mass		Without subcutaneous mass
Lumbosacral	Cervical	
Lipomyelocele	Meningocele[a]	Diastematomyelia
Lipomyelomeningocele	Myelocystocele	Caudal regression syndrome
Meningocele		Dermal sinus
Terminal myelocystocele		Intradural lipoma
		Filar lipoma
		Tight filum terminale
		Persistent terminal ventricle
		Dorsal enteric fistula
		Neurenteric cysts
		Segmental spinal dysgenesis

[a] Cervical meningocele can present with or without subcutaneous mass

also be seen. The spinal cord is low-lying in position (Fig. 2). Also seen is hypertrophy of subcutaneous fat; however, in contrast to lipomyelocele, the placode-lipoma interface in lipomyelomeningocele lies outside the spinal canal. There is characteristic widening of the subarachnoid CSF space. Thoracic lipomyelomeningocele is a rare variant (Fig. 2). In this anomaly, the neural placode is segmental, and the spinal cord distal to the placode shows normal MR morphology. The presence of placode-lipoma interface outside the canal and accompanying subarachnoid space widening in this case confirm the diagnosis of lipomyelomeningocele.

Meningocele

A classic lumbosacral meningocele shows herniation of a CSF-filled pachymeningeal sac through a posterior spinal defect (Fig. 3). The spinal cord might be low-lying but does not form a component of the sac (Fig. 3). Nerve roots, glial tissue, hypertrophic filum and fibrotic bands

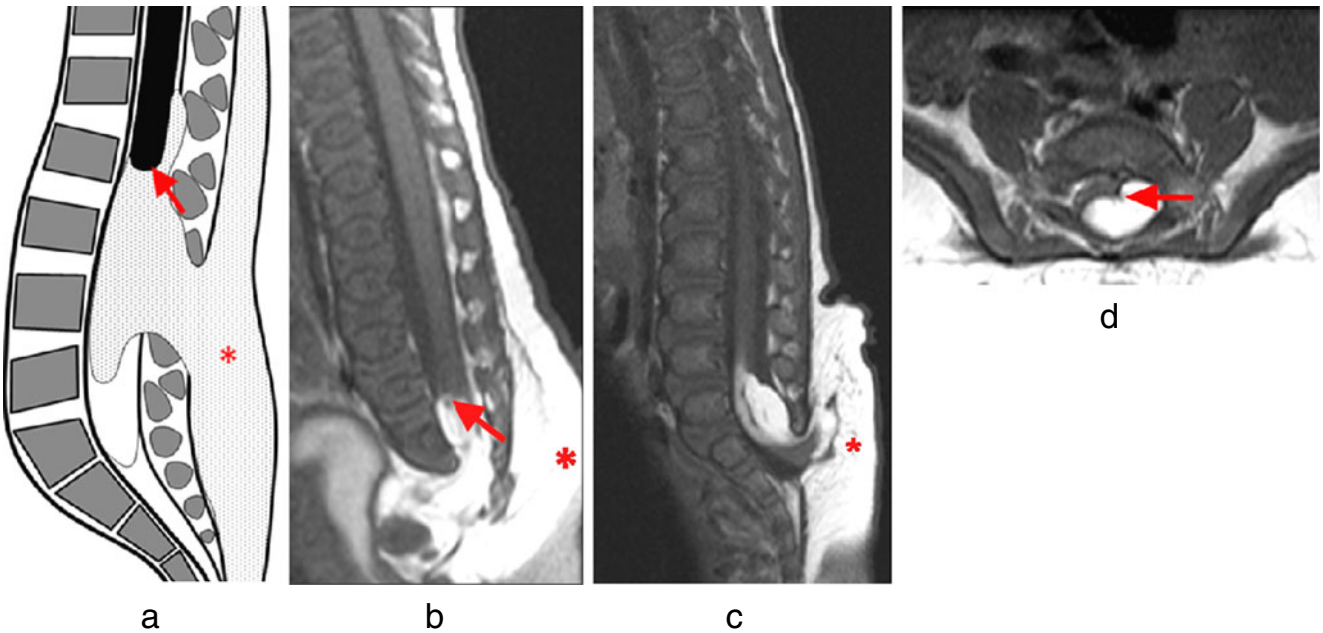

Fig. 1 Lipomyelocele. **a**, **b** Schematic representation and sagittal T1-W MR image of lipomyelocele. Placode-lipoma interface (*arrow*) lies within the spinal canal with lipomatous hypertrophy of subcutaneous fat (*asterisk*). Also note the distal sacral agenesis and low-lying cord (often coexistent). **c**, **d** Sagittal and axial T1-W images of another case of lipomyelocele. The placode-lipoma interface (*arrow*) can extend over several levels and is well evaluated on axial images

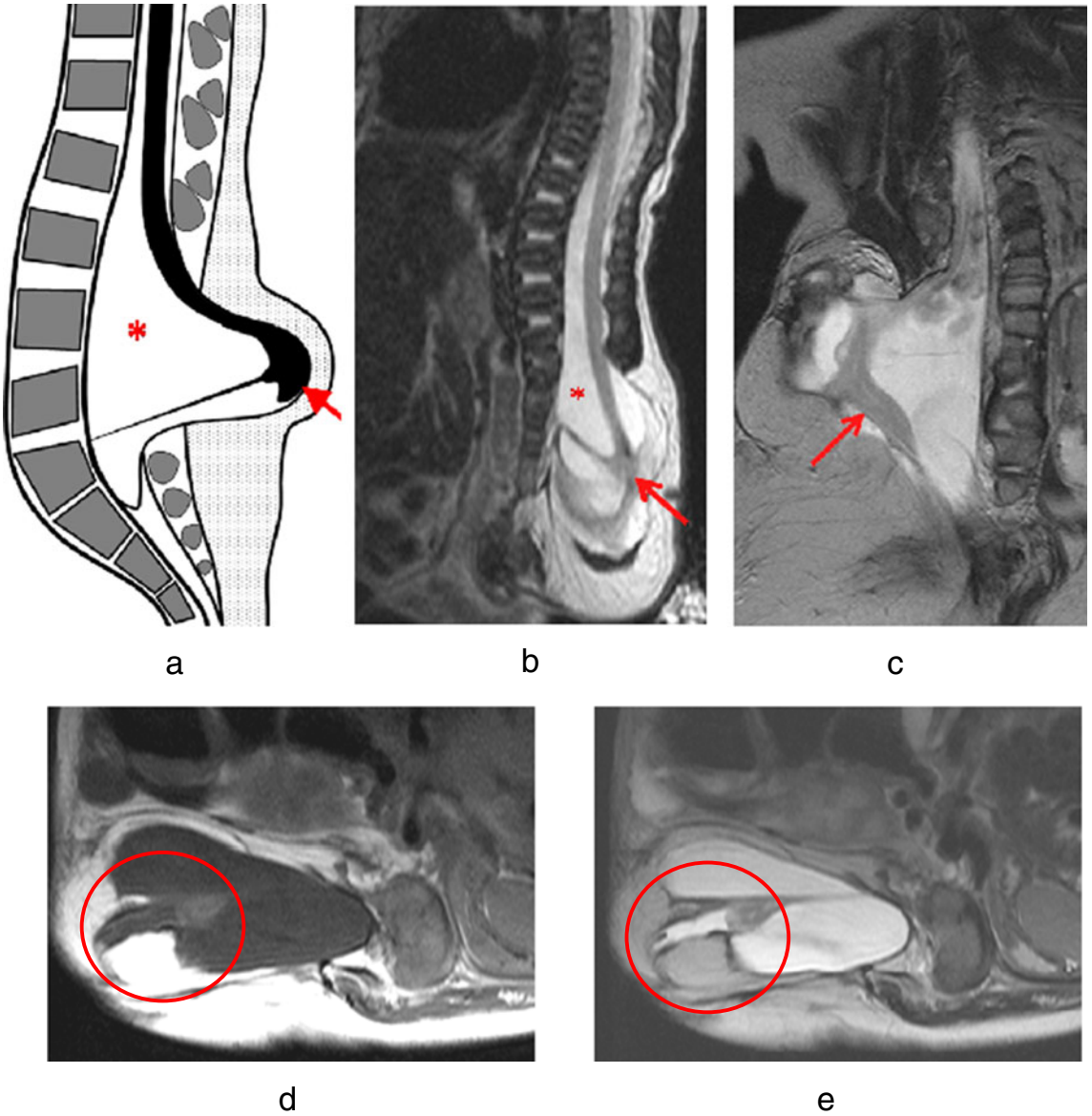

Fig. 2 Lipomyelomeningocele. **a**, **b** Schematic diagram and sagittal T2-W MR images of a lumbosacral lipomyelomeningocele. Note the widened subarachnoid space (*asterisk*) and placode-lipoma interface outside the spinal canal (*arrow*). **c**–**e** Coronal T2-W and axial T1-W and T2-W images of a thoracic lipomyelomeningocele. The spinal cord appears to regain normal morphology (*arrow*) beyond the segmental placode. Encircled in axial images is the placode-lipoma interface outside the spinal canal

might be present in the sac. There is no lipomatous hypertrophy of subcutaneous fat as in lipomyelocele and lipomyelomeningocele. Anterior presacral and intrasacral meningoceles are also seen occasionally (Fig. 3). Anterior presacral meningocele is closely associated with caudal regression. Intrasacral meningoceles should not be confused with Tarlov cysts, which extend into the neural foramina along the nerve roots. Anterior presacral and intrasacral meningoceles are exceptions to the classification followed herein as they do not present with a subcutaneous mass. Meningoceles can also be thoracic or cervical (discussed in a subsequent section) in location. Upper thoracic lateral meningocele also shows CSF-filled herniated sac of pachymeninges without involvement of the spinal cord (Fig. 3).

Terminal myelocystocele

The hallmark of a classic terminal myelocystocele is a low-lying spinal cord with cystic expansion of the caudal central canal extending outside the spinal canal (Fig. 4). The subarachnoid space surrounding this cyst is widened. There is no lipomatous hypertrophy of subcutaneous fat. Terminal myelocystoceles are associated with the OEIS complex (*o*mphalocele, cloacal *e*xstrophy, *i*mperforate anus and *s*pinal anomalies).

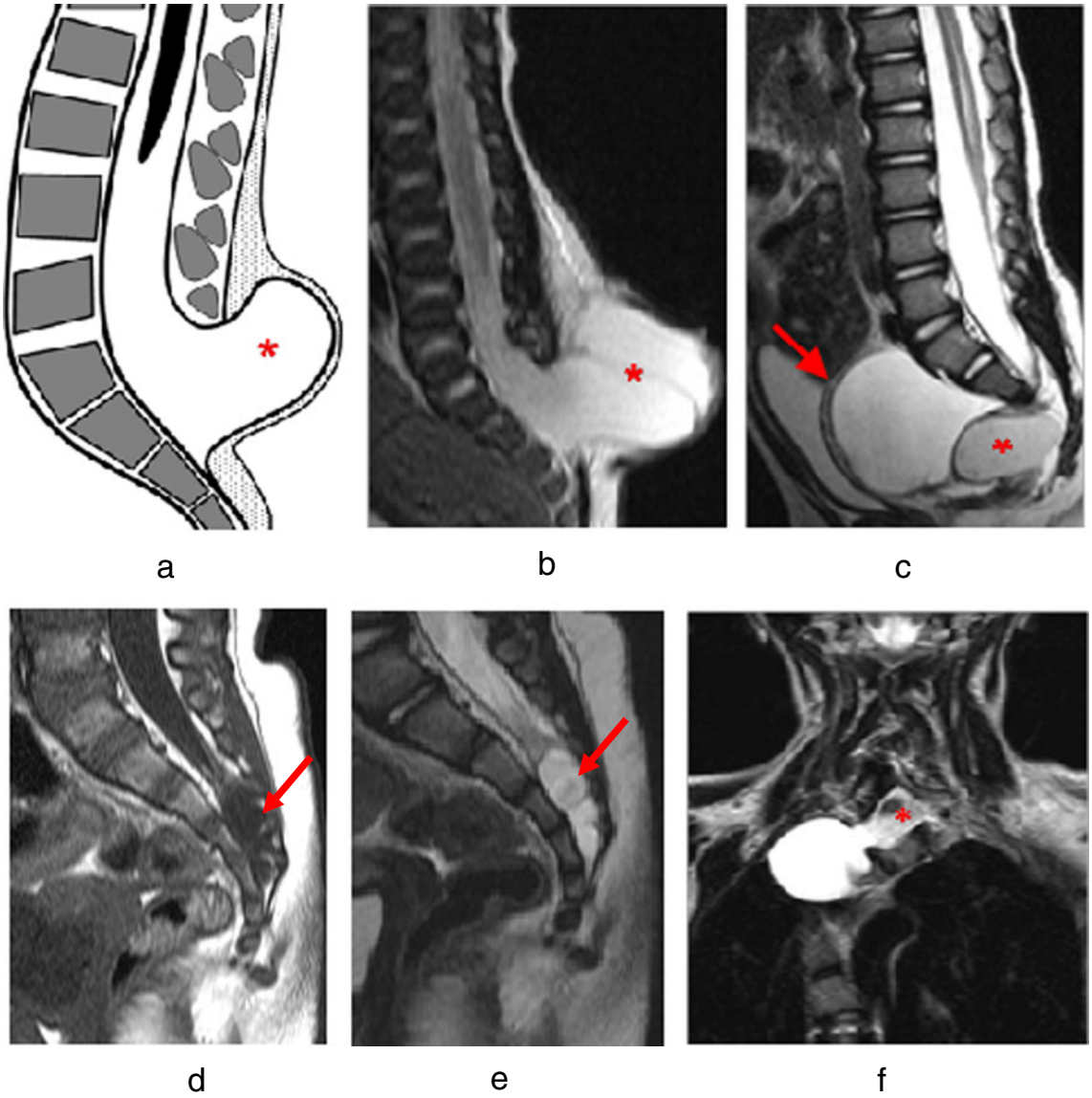

Fig. 3 Meningocele. **a**, **b** Schematic and sagittal T2-W MR images of a lumbosacral meningocele with herniation of the pachymeningeal sac (*asterisk*). **c** Sagittal T2-W image of anterior presacral meningocele with distal sacral agenesis. A definite wall (*arrow*) separates the anterior larger component from the urinary bladder. Smaller component (*asterisk*) shows slightly different signal. **d**, **e** T1-W and T2-W sagittal images of an intrasacral meningocele (*arrow*). **f** Coronal T2-W image of a lateral thoracic meningocele. The cord (*asterisk*) is not involved; there is no associated lipomatous hypertrophy of subcutaneous fat

Cervical closed spinal dysraphisms with subcutaneous mass

Meningocele and myelocystocele are the two anomalies included in this category.

Meningocele

Cervical meningocele shows herniation of a CSF-filled pachymeningeal sac through a posterior spinal defect. This pachymeningeal sac might contain fibrous and neuroglial elements; however, the spinal cord itself shows no evidence of distortion, tethering or hydromyelia (Fig. 5). An associated dermal sinus tract might accompany the meningocele (Fig. 5).

As indicated in Table 1, cervical meningocele can also present without a subcutaneous mass if the meningocele is small in size (Fig. 5).

Myelocystocele

Cervical myelocystocele is a form of nonterminal myelocystocele. Although cervical meningocele has morphological resemblance to its classic lumbosacral counterpart, cervical

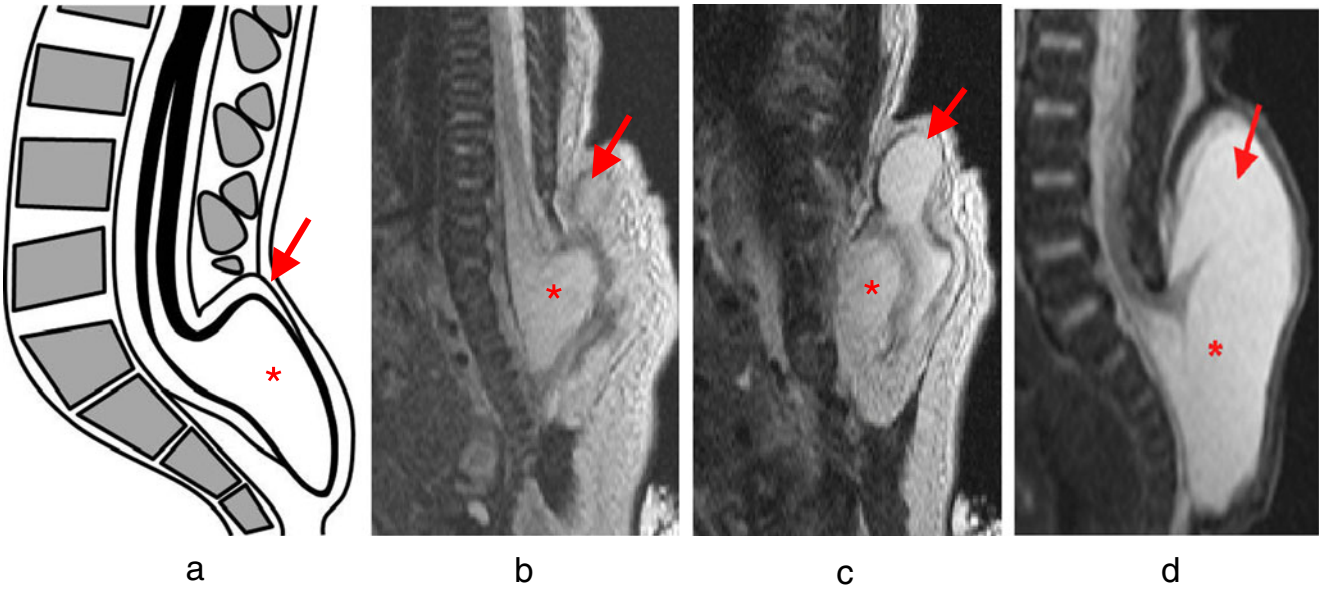

Fig. 4 Terminal myelocystocele. **a**–**c** Schematic representation and sequential sagittal T2-W MR images of a terminal myelocystocele. The caudal central canal forms an expansile sac (*asterisk*) that herniates into an outer meningocele (*arrow*). **d** Another case of terminal myelocystocele

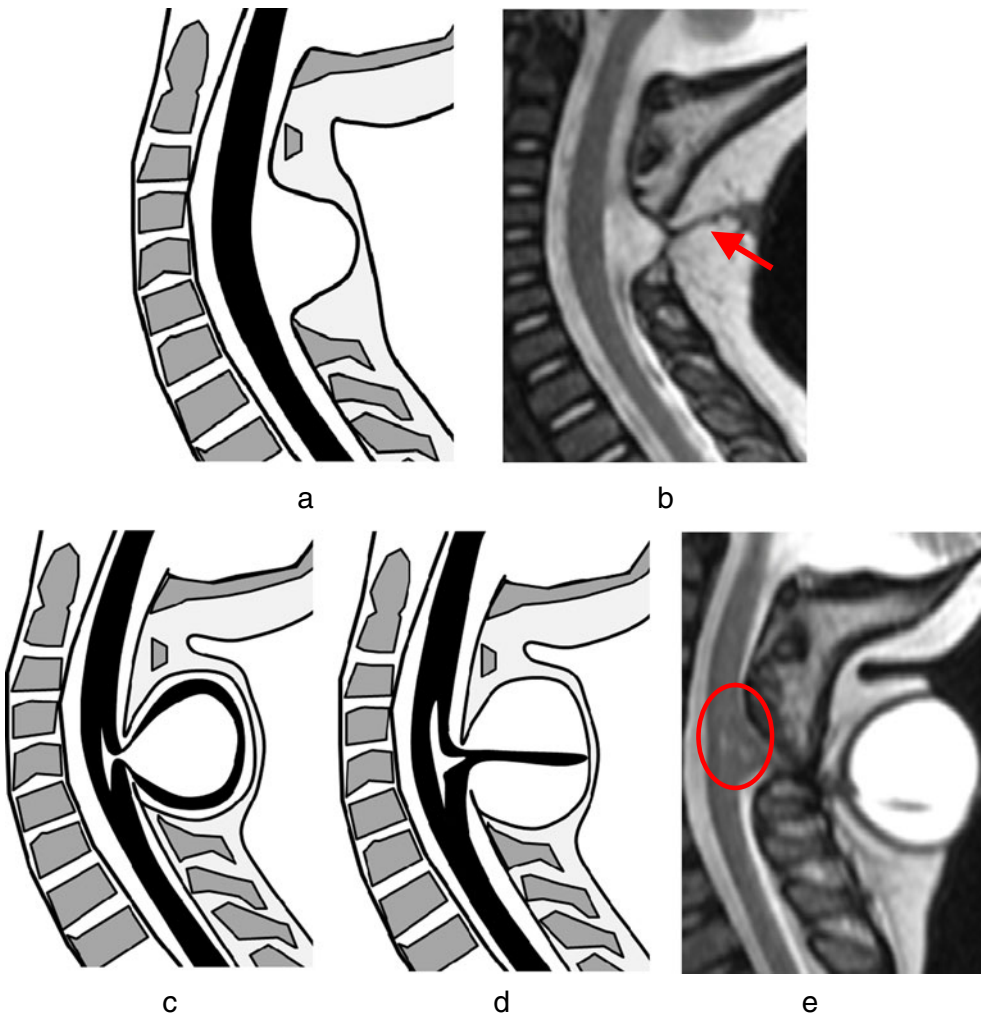

Fig. 5 Meningocele. **a**, **b** Schematic and sagittal T2-W MR images of a cervical meningocele. Note the intact spinal cord. An accompanying dermal sinus tract is seen in the MRI (*arrow*). **c** Schematic representation of a complete nonterminal myelocystocele with a typical cyst-within-cyst appearance. **d**, **e** Abortive cervical myelocystocele. Note the subtle T2-W bright signal in the cord (*encircled*) at the site of tethering in (**e**), suggesting focal hydromyelia

myelocystocele differs from lumbosacral myelocystocele in morphology as it involves a nonterminal portion of the spinal cord.

Based on cord morphology, nonterminal myelocystocele is classified as [16]:

(a) *Complete myelocystocele*, in which there is focal expansion of the central canal with stretching of the dorsal wall of the spinal cord. The wall herniates through a dorsal spinal defect into a widened subarachnoid space, giving the lesion a typical cyst-within-cyst appearance (Fig. 5).
(b) *Abortive myelocystocele* is characterized by the presence of a fibroneurovascular stalk, which arises from the dorsal surface of the cervical cord and attaches to the dome of a meningocele (Fig. 5). The stalk tethers and distorts the spinal cord at its attachment, which differentiates this lesion from a cervical meningocele. The cord also shows focal hydromyelia with a hint of CSF signal extending into the stalk, suggesting involvement of central canal and an abortive attempt to form a complete myelocystocele. Differences in opinion regarding nomenclature of cervical closed spinal dysraphisms persist, with some authors describing this lesion as cervical myelomeningocele [17–19]. It should be noted that the term "myelomeningocele" is also commonly used in context of open spinal dysraphisms, which are fundamentally different from the above-described skin-covered cervical lesions.

Closed spinal dysraphisms without subcutaneous mass

Lesions in this category are broadly classified based on cord morphology (i.e. truncation, splitting or abnormal elongation), presence or absence of intraspinal fat, and presence or absence of dermal sinus. Again there is considerable overlap of characteristics and two or more lesions often coexist, as we have shown in the cases below.

Diastematomyelia

In this malformation, the spinal cord is split into two hemi cords by a dividing septum. Two types of diastematomyelia are observed, differentiated by septal morphology:

(a) *Type I*: The two hemicords are encased in respective dural sacs and separated by a bony septum (Fig. 6). This anomaly most commonly occurs in the thoracolumbar region. There might be hydromyelia and tethering in one or both hemicords. In thoracic diastematomyelia, the hemicords tend to fuse again beyond the separation to form a normal spinal cord distally. In the lumbar region, the splitting is more elongated and the lumbar hemicords remain separated [14]. Severe vertebral segmentation and fusion anomalies, with resultant scoliosis, are typically observed along with type I diastematomyelia.
(b) *Type II*: The two hemicords are encased in a single dural sac and separated by a fibrous septum (Fig. 6). The fibrous septum is best visualized on axial T2-W images. Associated anomalies are less severe in type II than in type I diastematomyelia.

Caudal regression syndrome (CRS)

As the name suggests, this syndrome includes anomalies with distal spinal cord and vertebral agenesis. There is a strong association between prevalence of diabetes in mothers and the presence of CRS in neonates [20]. Two types of CRS are observed, distinguished by the severity of agenesis:

(a) *CRS type I*: The spinal cord typically shows a high abrupt cut-off accompanied by agenesis of distal vertebral column (Fig. 7). In general, the more proximal the cord cut-off, the more severe is the accompanying vertebral agenesis. Type I CRS is often associated with other anomalies such as anterior sacral meningocele, Currarino triad (partial sacral agenesis, anorectal malformations, presacral mass/teratoma) and VACTERL (*v*ertebral, *a*norectal, *c*ardiac, *t*racheo*e*sophageal, *r*enal and *l*imb) anomalies.
(b) *CRS type II*: This is a less severe form of caudal regression with mild agenesis of S2 and lower sacral vertebrae. The conus of the spinal cord is elongated, stretched and often tethered (Fig. 7).

Dermal sinus

A dermal sinus is an epithelium-lined tract extending inward from the skin surface, occurring most commonly in the lumbosacral region (Fig. 8). The sinus can communicate with the subarachnoid space, potentially leading to CSF leak, meningitis or abscess. Intraspinal lipomas, dermoids or hamartomas sometimes coexist. The spinal cord conus might be abnormally low-lying in position. A high sacral dimple, (i.e. located above the natal cleft), with an upward coursing dermal sinus tract is more frequently associated with the aforementioned complications [11].

Intradural lipoma

An intradural lipoma is caused by the abnormal separation of the neuroectoderm from surface ectoderm [11]. As a result,

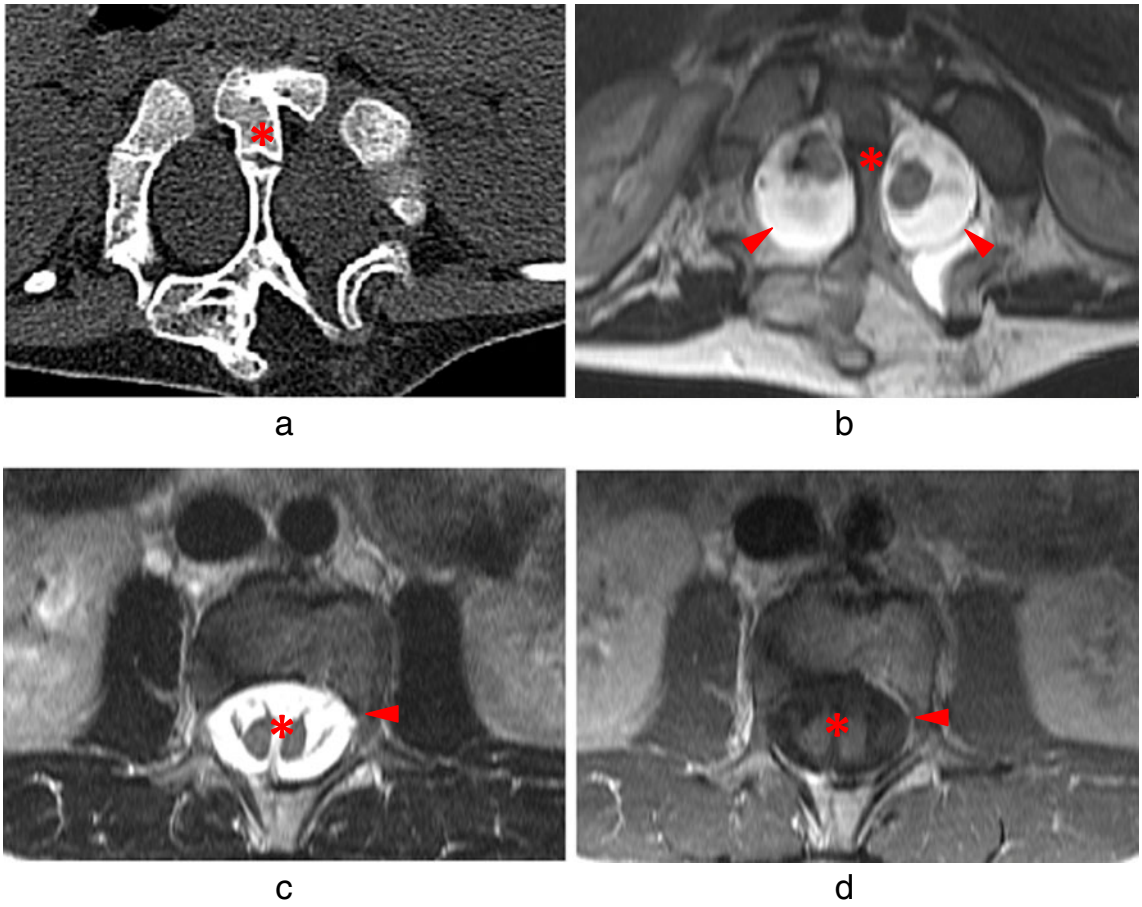

Fig. 6 Diastematomyelia. **a**, **b** Axial CT and axial T2-W MR images of type I diastematomyelia. Note the bony bar (*asterisk*) dividing the spinal canal with two hemicords encased in two separate dural sacs (*arrowheads*). **c**, **d** Axial T1-W and T2-W MR images of type II diastematomyelia with a fibrous septum (*asterisk*) dividing the spinal canal. Two hemicords are encased in single dural sac (*arrowhead*)

there is incorporation of fatty tissue inside the dural sheath (Fig. 9). The lipoma can be a solitary lesion or can coexist with a dermal sinus and caudal regression syndrome (Fig. 7).

Filar lipoma

The term filar lipoma refers to a filum that is both >2 mm in diameter and contains fat signal [14] (Fig. 10). If the thickened filum shows predominantly fibrous tissue and less fatty signal, then the term fibrolipoma is used. The fat infiltration can cause stretching and tethering of the conus resulting in neurological symptoms. Filar lipoma is a common cause of tethered cord syndrome (see below) [21]. However, filar fat can be seen incidentally in patients without any symptoms of cord tethering [22]. Filar lipoma can coexist with other intraspinal lipomas, dermoids and dermal sinuses.

Tight filum terminale (TFT)

TFT is characterized by a short, thickened, non-fatty filum causing tethering and impaired ascent of the conus medullaris [23] (Fig. 10). The filum thickness (or diameter) is usually measured on axial images at the level of L5-S1 [24]. In TFT, the thickened filum usually measures greater than 2 mm in diameter [14, 24]. In symptomatic cases where the filum measures less than 2 mm in diameter or subjectively appears normal, tethering caused by tight filum terminale cannot be excluded as the filar pathology might be beyond imaging resolution [25, 26].

Persistent terminal ventricle

Also known as the fifth ventricle, persistent terminal ventricle is a dilated, ependyma-lined cavity located within the conus (Fig. 11). This cavity is continuous with the central canal [27]. Mild forms are asymptomatic and usually considered normal variants; however, rare cases of large lesions causing neurological symptoms have also been reported [28]. A lack of enhancement and absence of any solid component differentiate this lesion from intramedullary tumors.

Dorsal enteric fistula, neurenteric cyst and segmental spinal dysgenesis are rare forms of closed spinal dysraphisms.

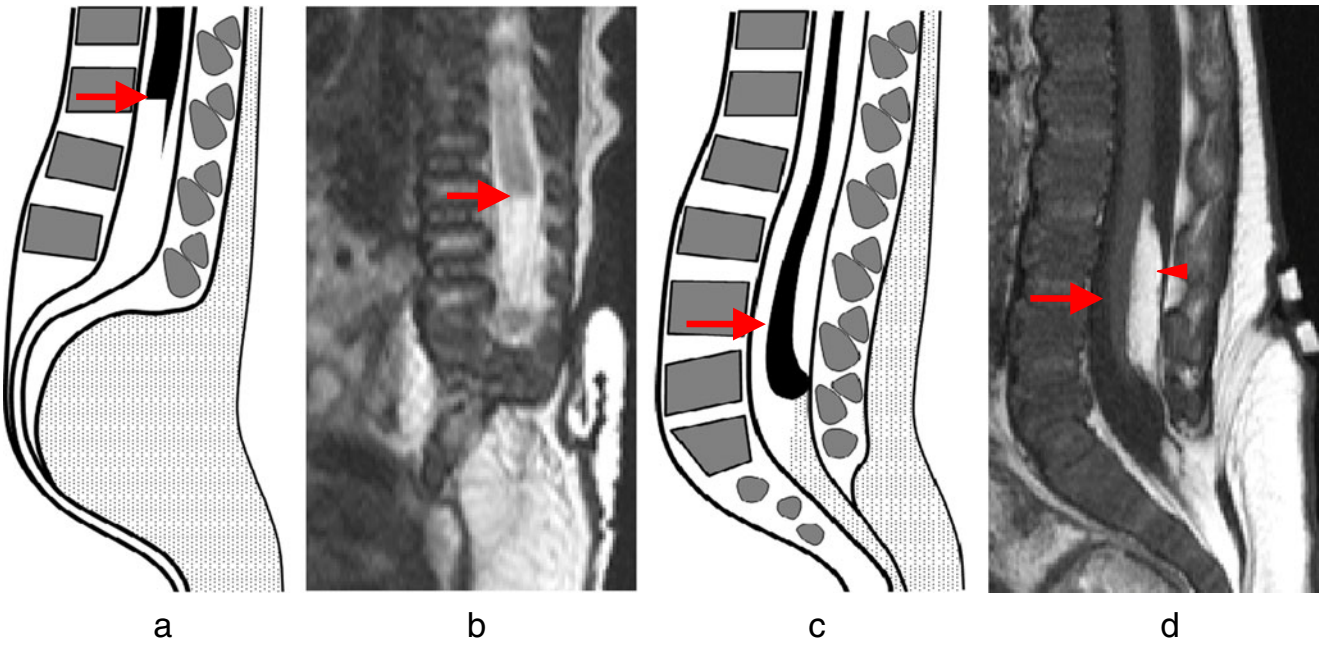

Fig. 7 Caudal regression syndrome. **a**, **b** Schematic and sagittal T2-W MR images of type I caudal regression syndrome, characterized by high abrupt cut-off of the spinal cord (*arrow*) and severe vertebral agenesis beyond that level. **c**, **d** Schematic and sagittal T1-W images of type II caudal regression syndrome. The spinal cord is abnormally elongated (*arrow*) with mild lower vertebral dysgenesis and distal sacral agenesis. Also noted in this case are a large intradural lipoma (*arrowhead*) and a dermal sinus with a cutaneous marker

These three lesions are known to have very specific morphological characteristics and the intent behind including their brief description here is to make readers aware of their key diagnostic features.

Dorsal enteric fistula

This entity is an epithelium-lined tract connecting a bowel loop to the dorsal midline skin surface. The fistulous tract

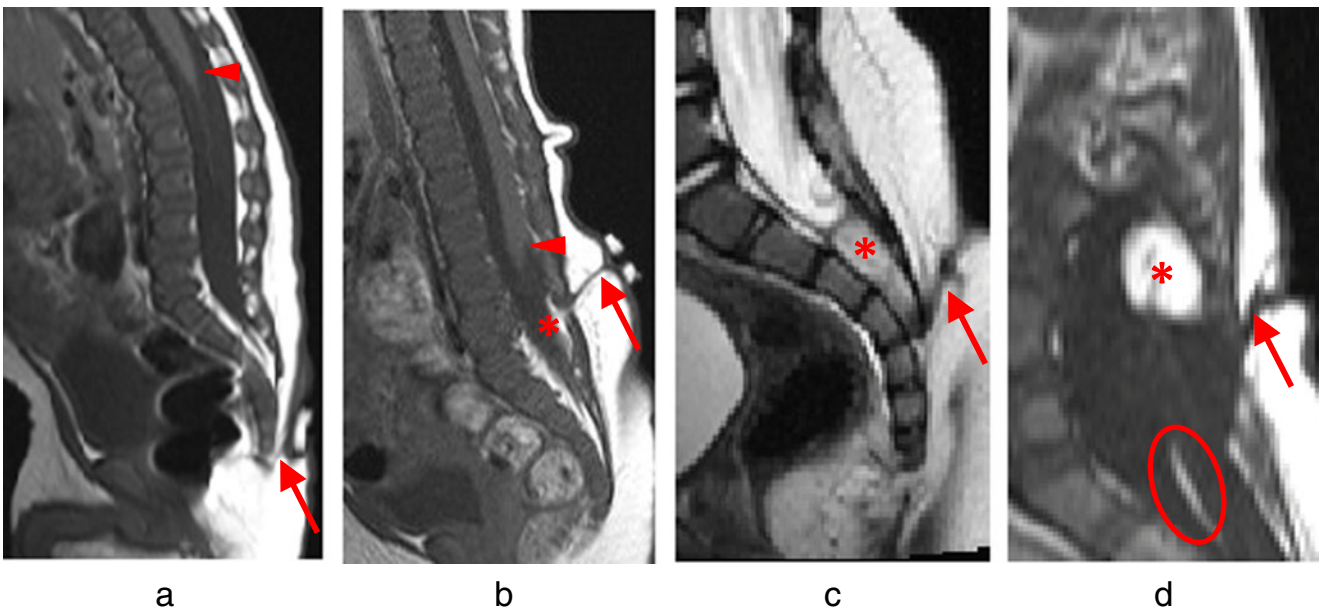

Fig. 8 Dermal sinus. **a** Sagittal T1-W MR image demonstrates a low-midline dermal sinus (*arrow*) with a cutaneous marker. The conus is normal in position (*arrowhead*) and there are no associated lesions. **b** Sagittal T1-W image of a dermal sinus (*arrow*) within a subcutaneous lipoma. Also seen is low-lying conus (*arrowhead*) and fatty filum terminale (*asterisk*). **c** Sagittal T2-W image of a dermal sinus (*arrow*) with a surgically proved intrasacral dermoid (*asterisk*). **d** Sagittal T1-W image of a dermal sinus (*arrow*) with an intradural lipoma (*asterisk*) and fatty filum (*circle*)

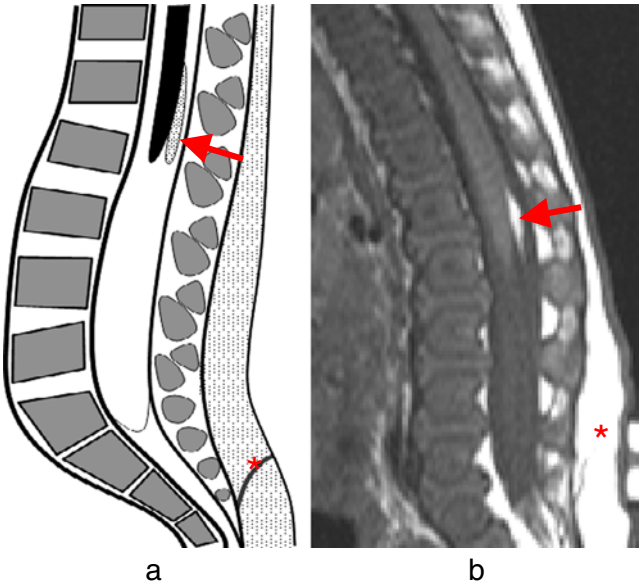

Fig. 9 Intradural lipoma. **a**, **b** Schematic and sagittal T1-W images of an intradural lipoma (*arrow*). Also noted is an associated dermal sinus (*asterisk*) with a cutaneous marker, which initiated evaluation in this child

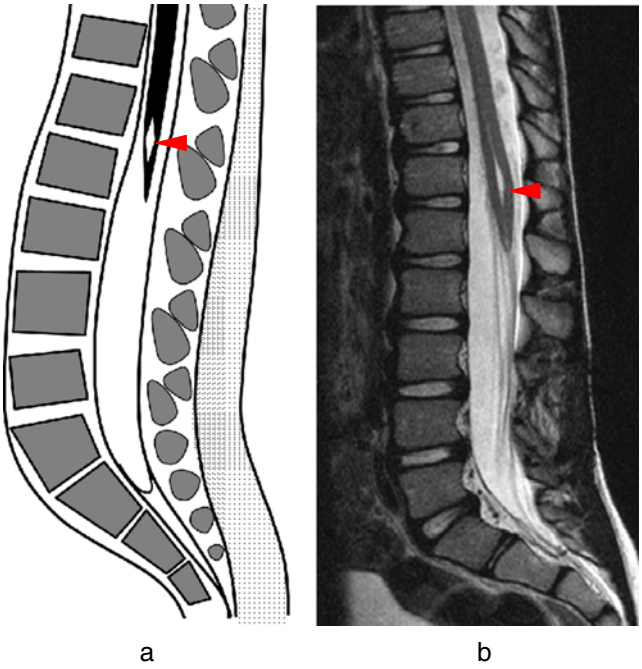

Fig. 11 Persistent terminal ventricle. **a**, **b** Schematic and sagittal T2-W images of the spinal cord with persistent terminal ventricle (*arrowhead*). The conus is otherwise normal in morphology and position

cleaves through the vertebral column and its contents, and through the subcutaneous tissue [11, 14].

Neurenteric cysts

These are congenital cysts lined by intestinal epithelium, found commonly in the cervico-thoracic region, usually ventral to the spinal cord in the intradural space. Rarely, these cysts are dorsal to the cord or intramedullary and exert mass effect on the spinal cord. On MRI, the cyst appears iso-hyperintense to CSF on T1-W images because of its high protein content and usually shows no post-contrast enhancement. Other spinal anomalies can coexist [29, 30].

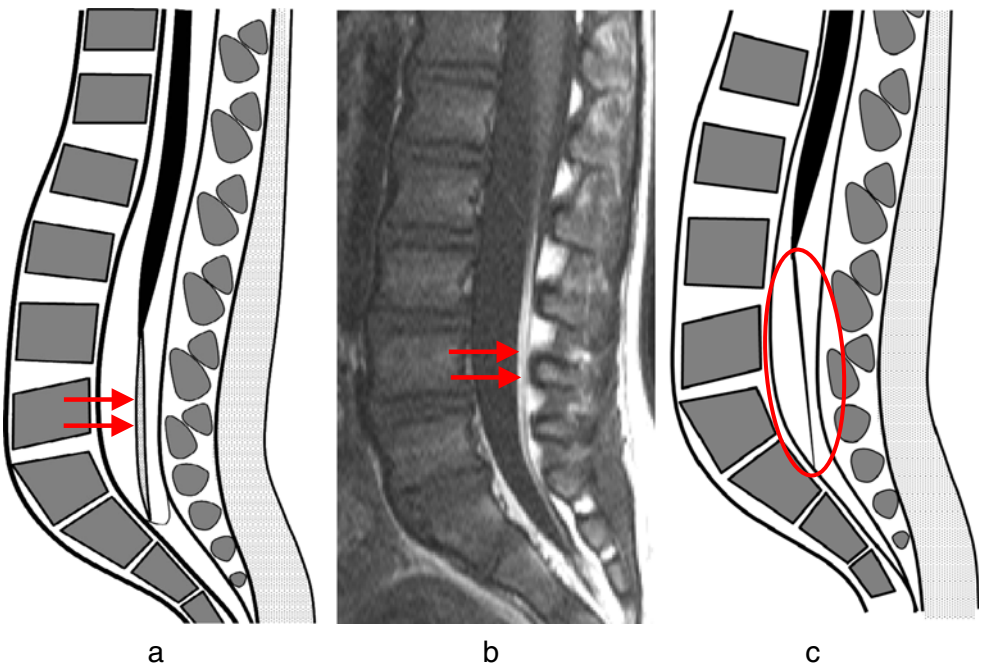

Fig. 10 Filar lipoma. **a**, **b** Schematic and sagittal T1-W MR images of filar lipoma (*arrows*) with no other abnormality. The conus is normal in position. **c** Schematic representation of tight filum terminale. Thickened filum terminale (*encircled*) and absence of fatty signal on MRI is characteristic

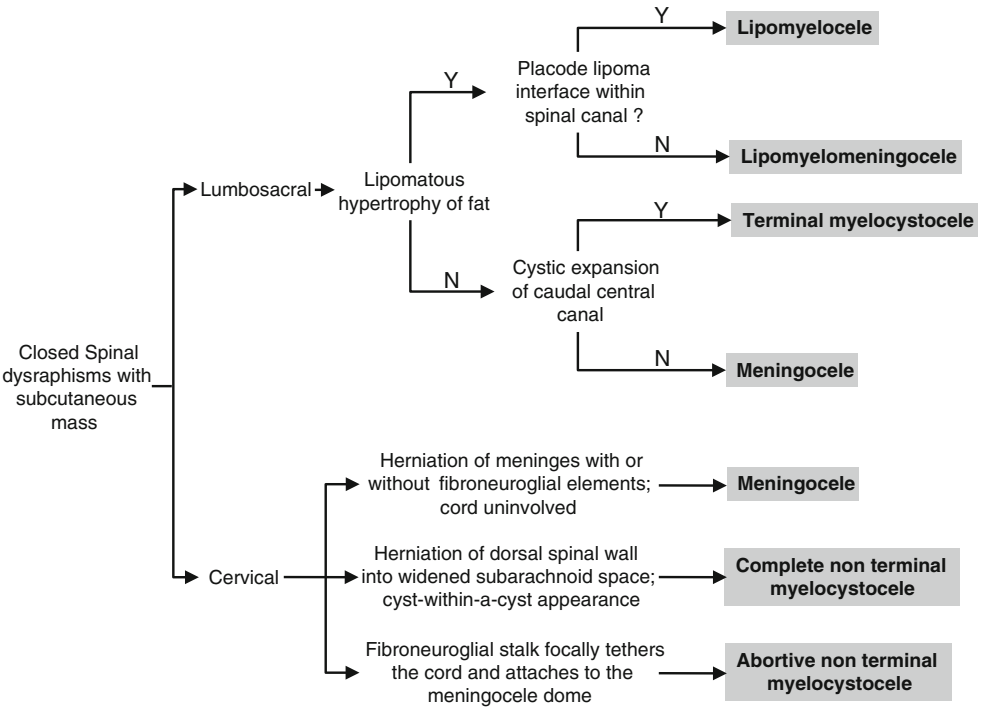

Fig. 12 Diagnostic algorithm of closed spinal dysraphism presenting with a subcutaneous mass

Segmental spinal dysgenesis (SSD)

SSD is characterized by segmental agenesis or dysgenesis of thoracolumbar spine as well as the spinal cord and nerve roots at the corresponding level. Severe spinal curvature abnormalities and lower limb anomalies might also be present [31].

Tethered cord syndrome (TCS)

The term tethered cord syndrome was coined by Hoffman [32] in 1976. TCS is a constellation of progressive neurological, gastrointestinal, urological and musculoskeletal symptoms caused by stretching and traction of the spinal cord. The most common tethering lesions include filar lipomas, dermoids, tight filum terminale, fibrosis, and post-surgical adhesions. The conus is usually, but not necessarily, low-lying [21]. MRI evaluation is vital in identifying the tethering lesion and the conus position.

Diagnostic approach to closed spinal dysraphisms

In this section, we outline a diagnostic approach to closed spinal dysraphisms based on the morphological imaging features described in the above case review. Figures 12

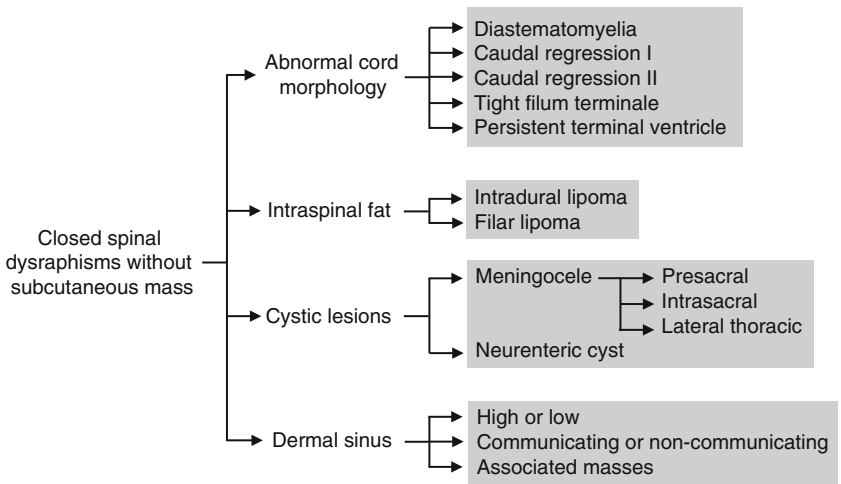

Fig. 13 Important diagnostic considerations in a patient of closed spinal dysraphism presenting without a subcutaneous mass

and 13 are diagnostic algorithms for the two main categories of closed spinal dysraphisms, i.e. with subcutaneous mass and without subcutaneous mass.

Closed spinal dysraphisms can be classified on the basis of their location into lumbosacral and cervical spinal dysraphisms (Fig. 12). In lumbosacral lesions lipomyelocele and lipomyelomeningocele can be distinguished based on hypertrophy of subcutaneous fat, position of placode-lipoma interface, and widening of the subarachnoid space. CSF-filled pachymeningeal herniation is seen in both meningocele and terminal myelocystocele; however, the latter also shows cystic expansion of the caudal central canal into the outer meningocele.

In cervical closed dysraphisms, herniation of pachymeninges without involvement of the spinal cord leads to the diagnosis of meningocele. The complete cervical nonterminal myelocystocele is characterized by a typical cyst-within-cyst appearance formed by herniation of the dorsal spinal wall into widened subarachnoid space. In abortive cervical nonterminal myelocystocele, the presence of a fibroneuroglial stalk causing focal cord tethering and hydromyelia leads to diagnosis.

In comparison to anomalies with subcutaneous mass, the classification of closed spinal dysraphisms without subcutaneous mass is more complex, involving the possibility of multiple coexisting lesions (Fig. 13). The important considerations in this category are degree of cord abnormality, presence or absence of intraspinal fat, location of intraspinal cystic lesion, and presence or absence of a dermal sinus. While cord abnormality can be extremely severe in diastematomyelia and CRS type I, it is extremely subtle and clinically insignificant in persistent terminal ventricle. The location of intraspinal fat differentiates intradural lipoma from filar lipoma. Meningocele can present without subcutaneous mass if it is lateral thoracic, presacral or intrasacral in location. Neurenteric cysts are uncommon lesions with a characteristic location and MRI appearance (as described above). The location and direction of the sinus tract, communication with the thecal sac, and presence of intraspinal masses (dermoid, lipoma or hamartoma) are important considerations in evaluating a case of dermal sinus.

Conclusion

Understanding the key embryological and imaging features of various types of closed spinal dysraphisms leads to an organized diagnostic approach for this complex group of anomalies. Genetic, neurosurgical and imaging studies on spinal dysraphisms continue to be the focus of several research efforts with current emphasis on prenatal diagnosis, prenatal therapy, postnatal management and improved long-term care.

References

1. Lichtenstein BW (1940) Spinal dysraphism: spina bifida and myelodysplasia. Arch Neurol Psychiatry 44:792–810
2. James CC, Lassman LP (1960) Spinal dysraphism: an orthopaedic syndrome in children accompanying occult forms. Arch Dis Child 35:315–327
3. Anderson FM (1975) Occult spinal dysraphism: a series of 73 cases. Pediatrics 55:826–835
4. Naidich TP, McLone DG, Mutluer S (1983) A new understanding of dorsal dysraphism with lipoma (lipomyeloschisis): radiologic evaluation and surgical correction. AJR 140:1065–1078
5. Barnes PD, Lester PD, Yamanashi WS et al (1986) MRI in infants and children with spinal dysraphism. AJR 147:339–346
6. Tortori-Donati P, Rossi A, Cama A (2000) Spinal dysraphism: a review of neuroradiological features with embryological correlations and proposal for a new classification. Neuroradiology 42:471–491
7. Au KS, Ashley-Koch A, Northrup H (2010) Epidemiologic and genetic aspects of spina bifida and other neural tube defects. Dev Disabil Res Rev 16:6–15
8. Shin M, Besser LM, Siffel C et al (2010) Prevalence of spina bifida among children and adolescents in 10 regions in the United States. Pediatrics 126:274–279
9. Centers for Disease Control and Prevention (CDC) (2009) Racial/ethnic differences in the birth prevalence of spina bifida - United States, 1995–2005. MMWR Morb Mortal Wkly Rep 57:1409–1413
10. Honein M, Paulozzi L, Matthews T et al (2001) Impact of folic acid fortification of the US food supply on the occurrence of neural tube defects. JAMA 285:2981–2986
11. Tortori-Donati P, Rossi A, Biancheri R et al (2001) Magnetic resonance imaging of spinal dysraphism. Top Magn Reson Imaging 12:375–409
12. Kaplan KM, Spivak JM, Bendo JA (2005) Embryology of the spine and associated congenital abnormalities. Spine J 5:564–576
13. Cabaret AS, Loget P, Loeuillet L et al (2007) Embryology of neural tube defects: information provided by associated malformations. Prenat Diagn 27:738–742
14. Rossi A, Gandolfo C, Morana G et al (2006) Current classification and imaging of congenital spinal abnormalities. Semin Roentgenol 41(4):250–273
15. Rossi A, Cama A, Piatelli G et al (2004) Spinal dysraphism: MR imaging rationale. J Neuroradiol 31:3–24
16. Rossi A, Piatelli G, Gandolfo C et al (2006) Spectrum of nonterminal myelocystoceles. Neurosurgery 58:509–515
17. Pang D, Dias MS (1993) Cervical myelomeningoceles. Neurosurgery 33:363–372, discussion 372–373
18. Huang SL, Shi W, Zhang LG (2010) Characteristics and surgery of cervical myelomeningocele. Childs Nerv Syst 26:87–91
19. Ali MZ (2010) Cystic spinal dysraphism of the cervical region: experience with eight cases including double cervical and lumbosacral meningoceles. Pediatr Neurosurg 46:29–33
20. Dunn V, Nixon G, Jaffe R et al (1981) Infants of diabetic mothers: radiographic manifestations. AJR 137:123–128
21. Hertzler DA 2nd, DePowell JJ, Stevenson CB et al (2010) Tethered cord syndrome: a review of the literature from embryology to adult presentation. Neurosurg Focus 29:E1

22. Brown E, Matthes J, Bazan C et al (2004) Prevalence of incidental intraspinal lipoma of the lumbosacral spine as determined by MRI. Spine 19(7):833–836
23. Rossi A, Gandolfo C, Cama A et al (2007) Congenital malformations of the spine, spinal cord, and craniocervical junction. In: van Goethem J, Hauwe L, Parizel P (eds) Spinal imaging: diagnostic imaging of the spine and spinal cord. Springer, Berlin, pp 3–42
24. Raghavan N, Barkovich AJ, Edwards M et al (1989) MR imaging in the tethered spinal cord syndrome. AJR 152:843–852
25. Yundt K, Park T, Kaufman B (1997) Normal diameter of filum terminale in children: in vivo measurement. Pediatr Neurosurg 27:257–259
26. Nazar G, Casale A, Roberts J et al (1995) Occult filum terminale syndrome. Pediatr Neurosurg 23:228–235
27. Coleman LT, Zimmerman RA, Rorke LB (1995) Ventriculus terminalis of the conus medullaris: MR findings in children. AJNR 16:1421–1426
28. Sigal R, Denys A, Halimi P et al (1991) Ventriculus terminalis of the conus medullaris: MR imaging in four patients with congenital dilatation. AJNR 12:733–737
29. Shenoy SN, Raja A (2004) Spinal neurenteric cyst. Report of 4 cases and review of the literature. Pediatr Neurosurg 40:284–292
30. Cai C, Shen C, Yang W et al (2008) Intraspinal neurenteric cysts in children. Can J Neurol Sci 35:609–615
31. Tortori-Donati P, Fondelli MP, Rossi A et al (1999) Segmental spinal dysgenesis: neuroradiologic findings with clinical and embryologic correlation. AJNR 20:445–456
32. Hoffman HJ, Hendrick EB, Humphreys RP (1976) The tethered spinal cord: its protean manifestations, diagnosis and surgical correction. Childs Brain 2:145–155